RESEARCH ARTICLE

BON VIEW PUBLISHING

Multitarget-Directed Multiple Ligands in Anti-VEGF Resistant Glioblastoma Therapeutics: An in Silico Approach to Identify Potential Phytochemicals

Kesavan R. Arya[1] , Sasikumar J. Soumya[1], Anuroopa G. Nadh[1] , Thankamani R. Aswathy[1], Vijayalakshmi B.[1], Achuthsankar S. Nair[1], Oommen V. Oommen[1] and Perumana R. Sudhakaran[1,*]

[1]*Department of Computational Biology and Bioinformatics, University of Kerala, India*

Abstract: Angiogenesis is an important process in tumor progression. Vascular endothelial growth factor (VEGF) is the key factor regulating angiogenesis, and hence, anti-VEGF therapy is considered a useful therapeutic approach in tumor conditions. However, the drug resistance and lack of efficacy of existing drugs limit the potential of such a therapeutic approach in certain cases, and the tumor growth will continue through alternative mechanisms. Glioblastoma (GBM) is one such type of tumor that shows resistance to anti-VEGF therapy. Previously, we identified the hub genes differentially expressed in anti-VEGF resistance in GBM. Medhya Rasayana, an Ayurvedic formulation, is used for the management of neurological disorders. In the present study, we used computational docking methods to identify the phytochemicals present in the medicinal plants of Medhya Rasayana, which can target the proteins expressed by the hub genes associated with anti-VEGF resistance. Network pharmacological analysis was also performed to identify the highly effective phytochemicals for a possible adjuvant therapy. Results showed that multiple phytochemicals of Glycirrhiza glabra Linn, Evolvulus alsinoides, and Celastrus paniculatus target the anti-VGEF resistant proteins in GBM. This indicates the multi-targeting property of phytocompounds of Medhya Rasayana plants, which may be considered for adjuvant therapy along with anti-VEGF therapy.

Keywords: glioblastoma, transcriptome data analysis, angiogenesis, anti-VEGF therapy, drug resistance, molecular docking, Medhya Rasayana

1. Introduction

Angiogenesis is the formation of new blood vessels from existing vessels which supports the growth of tissues. It is crucial for the progression and metastasis of cancer. Since tumor tissue demands neovascularization to receive oxygen and nutrients for growth and metastasis, cancer cells trigger excessive angiogenesis [1]. Antiangiogenic therapy is a useful treatment option in cancer conditions. Vascular endothelial growth factor (VEGF) is the important growth factor regulating angiogenesis, and therefore, it is one of the prominent targets for anti-cancer therapeutics. Monoclonal antibodies targeting VEGF and VEGFR2 have been approved and used for the treatment of cancer. However, a significant issue in the anti-VEGF treatment of cancer is the development of resistance to anti-VEGF therapy [2, 3].

Glioblastoma (GBM) is the most common malignant primary brain tumor in adults and invariably carries a dismal prognosis. Despite current treatment approach like surgical resection followed by radiation therapy with adjuvant temozolomide, only 26–33%, 2-year survival rate is reported [4]. Further, recurrence of the disease is inevitable and salvage chemotherapies are largely ineffective [5]. Poor treatment response is attributed to intertumoral and intratumoral heterogeneity, de novo and acquired resistance, ineffective drug delivery as a result of blood-brain barrier (BBB), and multiple redundant cellular pathways regulating cellular survival and proliferation [6].

Bevacizumab, a humanized monoclonal antibody against VEGF, blocks angiogenesis and thereby reduces tumor growth in a variety of GBM mouse models. These preclinical studies and further clinical investigations led to approval of bevacizumab for the treatment of recurrent GBM [7]. However, a meta-analysis of clinical trials demonstrated that the addition of bevacizumab to standard chemo-radiotherapy only improves progression-free survival, with no improvement in overall survival (OS). The lack of durable response in the antiangiogenic therapy might be due to drug resistance which has prompted efforts to understand the mechanisms underlying this resistance. Adaptive and intrinsic resistance are the primary modes of resistance to antiangiogenic therapy [6]. Therapeutic approaches can be improved by elucidating the mechanism underlying drug resistance.

In GBM cells resistant to anti-VEGF therapy, angiogenesis is induced through alternate pathways converging to downstream of

*Corresponding author: Perumana R. Sudhakaran, Department of Computational Biology and Bioinformatics, University of Kerala, India. Emails: prsudhakaran@keralauniversity.ac.in; prslab@gmail.com

VEGF signaling pathways as indicated by differential expression of several genes. In our previous study [8], we identified the hub genes related to GBM resistance to anti-VEGF therapy using computational analysis of the gene expression data. Considering the lack of efficacy of the existing drugs, it would be worthwhile to search for alternative approach to find potent drugs with better efficacy to target the identified hub gene products.

Recent research focuses on identifying natural compounds that can modulate biological processes underlying disease condition. Therefore, we have employed Ayurvedic knowledge, Ayurinformatics-inspired approach to identify phytocompounds of medicinal plants that can target angiogenesis process. In the traditional Indian system of Ayurveda, a group of medicinal plants has been classified as "Medhya Rasayana" which offers benefits to improve memory and intellect and is known to be beneficial for various neurological disorders [9]. Medhya Rasayana consists of 13 medicinal plants; Centella asiatica, Glycyrrhiza glabra, Tinospora cordifolia, Canscora decussate, Clitoria ternatea, Convolvulus pluricaulis choisy, Evolvulus alsinoides, Bacopa monnieri, Acorus calamus; Plumbago zeylanica, Benincasa hispida, Celastrus paniculatus, and Nardostachys jatamansi.

In the present study, the possible inhibitory potential of the phytochemicals of Medhya Rasayana plants to target angiogenesis in anti-VEGF resistance in GBM has been analyzed using computational tools such as molecular docking and network pharmacology. Specifically, the phytocompounds targeting the proteins expressed by the hub genes differentially expressed in anti-VEGF resistance have been studied, and the results are presented below.

2. Materials and Methods

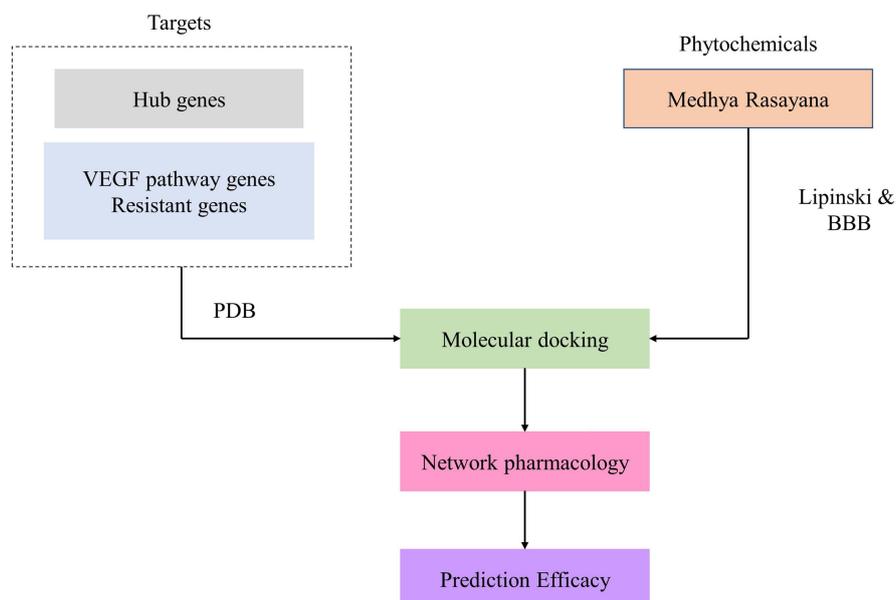The methodology workflow is presented in Figure 1.

2.1. Molecular docking

For target selection in docking studies, the proteins expressed by the hub genes, resistant genes, and potent genes in VEGF/VEGFR2 pathway were focused [8, 10]. The X-ray crystallographic structures of selected targets were retrieved from protein data bank (PDB). The raw protein structures were further prepared for docking studies by removing ligands, hetero atoms, and water molecules and adding hydrogen to polar groups using Discovery Studio Client v21.1.0.20298 (DS). For ligand preparation, the phyto profiles of the thirteen plants in Medhya Rasayana were selected from the internal library maintained by the Dept. of Computational Biology and Bioinformatics, University of Kerala, India; their chemical structures were retrieved from PubChem compound database. These phytochemicals were filtered using Lipinski's rule of five and BBB penetration potential [11, 12]. The resulting phytochemicals were prepared for the docking studies using DS. The target proteins were docked against phytocompounds using the LibDock protocol of DS for exploring the protein-ligand interactions.

2.2. Network pharmacological analysis

The plant-phytochemical-target interaction network was constructed using Cytoscape 3.7.1, in order to identify the highly effective plant/phytochemical for a possible adjuvant therapy. From the docking analysis of 557 phytocompounds with hub genes, resistant genes, and VEGF pathway genes, the top-scoring phytocompounds in each of the 13 plants were selected and constructed a network.

2.3. Calculation of prediction efficacy (PE)

PE is calculated to understand the therapeutic potential of a phytochemical in the anti-VEGF-resistant condition.

Figure 1. Flowchart of methodology

The PE of a phyto chemical compound was calculated by summing up its LibDock scores with all the targets obtained by docking with DS.

$$PE \ (Compound) = \Sigma score(TL),$$

where TL is the target-ligand complex.

Similarly, the PE of the Ayurvedic formulation was defined as the sum of PE of all the compounds contained in this Ayurvedic formulation

$$PE \ (Medhya \ Rasayana) = \Sigma score \ N(TL),$$

where N = highest docking score for each protein-ligand complex and TL is the target-ligand complex.

3. Results

3.1. In silico identification of phytochemical-protein interaction using molecular docking analysis

The ligands for the study were selected from the library of phytochemicals from Medhya Rasayana plants. A total of 1973 phytochemicals present in 13 medicinal plants of Medhya Rasayana were taken, of which 144 compounds were from Centella asiatica; 217 from Glycyrrhiza glabra; 204 from Tinospora cordifolia; 29 from Canscora decussate; 74 from Clitoria ternatea; 40 from Convolvulus pluricaulis Choisy; 168 from Evolvulus alsinoides; 104 from Bacopa monnieri; 488 from Acorus calamus; 126 from Plumbago zeylanica; 75 from Benincasa hispida; 65 from Celastrus paniculatus; 239 from Nardostachys jatamansi. The phytochemicals were filtered based on Lipinski's rule of five, and BBB parameters were calculated using the "ADMET" protocol of DS. Out of 1973 phytochemicals from Medhya Rasayana, 811 passed Lipinski's rule, and among these filtered phytochemicals, 642 passed BBB penetration. Among these 642 phytochemicals, 69 compounds were found in more than one plant so the duplications were removed, and the remaining 557 were selected.

The proteins associated with the hub genes differentially expressed in GBM resistance to anti-VEGF therapy were selected as targets [8]. The targets were categorized into three sets as follows: (1) Proteins expressed by 32 up-regulated hub genes; (2) genes involved in the formation of alternate pathways in anti-VEGF resistance condition (resistant genes), and the corresponding 41 proteins were selected as targets; (3) VEGF signaling pathway being one of the key pathways mediating angiogenesis and the effect of the Medhya Rasayana on 27 potent targets of VEGF signaling pathway were also examined. From these three sets, duplications were eliminated, and in total, 71 targets were selected for docking analysis. Genes which belong to the category of enzymes, receptors, hub, ligands, and the genes involved in alternate pathway are the criteria for the selection of resistant targets. Good quality crystal structures with a resolution below 3 Å were selected.

A total of 557 phytochemicals from Medhya Rasayana plants were docked against 71 target proteins. The binding site was set according to PDB site records. The mean LibDock score was calculated from the docking results, and a threshold value (LibDock score>=46.5) was set to filter out the docked pairs. Eleven compounds failed to form any pose in docking with any of the 71 targets. The results are categorized based on the target gene set and described below.

3.1.1. Molecular docking of phytochemicals with hub gene proteins

Thirty-two hub genes selected for the study were docked against 557 phytochemicals from Medhya Rasayana plants. The total number of phytochemicals docked against each target ranged from a minimum of 40 to a maximum of 551.

The phytochemical that gave the top docking score for each hub gene target is shown in Table 1. Out of 557 phytochemicals, 17 showed highest docking score with the 32 hub genes. The phytochemical with PubChem ID 569889 interacts with 13 targets (ALDOA, ATP2A2, CYP1B1, EGFR, IDH1, ITGAX, JAK1, NAMPT, NT5E, PLAUR, PLOD2, PTGS2, and TXNRD1); the phytochemical with PubChem ID 197678 interacts with 3 targets (ALDH1A13, HMOX1, THBS1); the compound with PubChem ID 54680871 interacts with 2 targets (RHOQ, VEGFA). The remaining 14 phytochemicals interact with 1 target each.

Also, for few targets, standard ligands were identified and were analyzed their molecular interaction; for ALDH1A13, the reference drug was disulfiram (PubChem ID 3117) which docked with a LibDock score of 69.38, which was less than that of the identified compound. In the case of EGFR, the reference drug was erlotinib (PubChem ID 176870) which showed LibDock score of 94.44; the identified phytocompound gave better docking score than the reference drug. For VEGFA, the reference drug was sunitinib (PubChem ID 5329102) which showed LibDock score of 88.05; the identified compound showed lower docking score than the reference drug. For PTGS2, the reference drug was rofecoxib (PubChem ID 5090) which showed the LibDock score of 116.03; the identified compound gave less docking score than the reference.

3.1.2. Molecular docking of phytochemicals with proteins of resistant genes involved in the formation of alternate pathway

Out of 41 target proteins identified to be involved in the formation of alternate pathways in anti-VEGF resistance, 25 genes were included in the hub gene list indicated above and the remaining 16 are included in this section. These 16 target proteins were docked against 557 phytochemicals from Medhya Rasayana plants.

The total number of phytochemical docked against each target ranges from 18 to 551. The phytochemical that gave the top docking score for each resistant gene target is shown in Table 1. 8 out of 557 phytochemicals gave top LibDock score with the 15 targets. The phytochemical with PubChem ID 569889 interacted with 7 targets viz. ACVR1, F3, FYN, IL11, NRP2, ZAK, and FGF13; the phytochemical with PubChem ID 442774 docked to targets LY96, RIPK2, and that with PubChem ID 31 docked to 2 targets (ITGA2, TIMP1), and the other 5 phytochemicals interact with 1 target each. Also, for one target ACVR1, the reference drug was nilotinib (PubChem ID 644241) which showed the LibDock score of 93.30; the identified compound showed better docking score than the reference drug.

3.1.3. Molecular docking of phytochemicals with proteins of VEGF pathway genes

Among 27 targets identified in VEGF signaling pathway, 2 genes were included in the hub gene list and 2 genes were included in the resistant gene list, and the remaining 23 targets were docked against 557 phytochemicals from Medhya Rasayana plants.

Table 1. Molecular docking of phytochemicals with targets identified in anti-VEGF-resistant glioblastoma

PubChem ID	Target	Plant name	LibDock score
HUB GENES			
965	IL1B	Bacopa monniera	73.89
235711	TGM2	Bacopa monniera	94.73
3689	IL6R	Evolvulus alsinoides	121.42
7991	LOX	Convolvulus pluricaulis Choisy	51.62
10256	IL6ST	Plumbago zeylanica	76.70
15608	SRC	Evolvulus alsinoides	77.24
18016	FGF2	Evolvulus alsinoides	79.30
39378	CD44	Glycirrhiza glabra Linn	79.93
92776	SERPINE1	Acorus calamus	71.44
442774	RARB	Glycirrhiza glabra Linn	156.83
581589	HSPA1B	Evolvulus alsinoides	104.58
5364942	CXCL8	Acorus calamus	77.26
5463146	HIF1A	Acorus calamus	56.06
131753027	ITGB1	Glycirrhiza glabra Linn	143.62
197678	(a)ALDH1A13, (b)HMOX1, (c)THBS1	Glycirrhiza glabra Linn	(a)133.53, (b)132.82, (c)125.03
569889	(a)ALDOA, (b)ATP2A2, (c)CYP1B1, (d) EGFR, (e)IDH1, (f)ITGAX, (g)JAK1, (h) NAMPT, (i)NT5E, (j)PLAUR, (k)PLOD2, (l)PTGS2, (m)TXNRD1	Celastrus paniculatus	(a)135.36, (b)151.02, (c)150.21, (d)148.13, (e)148.62, (f)115.73, (g)142.49, (h)135.09, (i)134.38, (j)163.06, (k)156.36, (l)136.74, (m)165.10
54680871	(a)RHOQ, (b)VEGFA	Bacopa monniera	(a)76.65, (b)76.36
RESISTANT GENES			
131753027	PTPRR	Glycirrhiza glabra Linn	117.02
20146588	MMP3	Plumbago zeylanica	88.11
6427087	FLNC	Glycirrhiza glabra Linn	49.44
600601	IL1A	Acorus calamus	79.21
581589	PDGFRB	Evolvulus alsinoides	90.53
569889	(a)ACVR1, (b)F3, (c)FYN, (d)IL11, (e)NRP2, (f)ZAK, (g)FGF13	Celastrus paniculatus	(a)130.85, (b)98.17, (c)129.18, (d)112.59, (e)133.82, (f)153.67, (g)130.85
442774	(a)LY96, (b)RIPK2	Glycirrhiza glabra Linn	(a)110.72, (b)148.06
31	(a)ITGA2, (b)TIMP1	Tinospora cordifolia	(a)62.60,(b)91.09
VEGF PATHWAY GENES			
538501	AKT	Acorus calamus	80.63
31	PKC Y	Tinospora cordifolia	57.29
18016	PXN	Evolvulus alsinoides	50.92
61290	RAF1	Acorus calamus	54.46
97790	MMP9	Evolvulus alsinoides	88.98
114829	NRP1	Glycirrhiza glabra Linn	80.24
5352449	CDC42	Celastrus paniculatus	110.00
5363633	RAS	Plumbago zeylanica	96.53
6452096	Hsp27	Benincasa hispida	116.59
5312513	PLC Y	Bacopa monniera	104.11
197678	(a)MAPK, (b)PI3K	Glycirrhiza glabra Linn	(a)131.57, (b)139.19
442774	(a)p38, (b)VEGFR2	Glycirrhiza glabra Linn	(a)140.90, (b)137.49
569889	(a)eNOS, (b)ERK, (c)FAK, (d)GSK 3β, (e) MEK, (f)VEGFR1, (g) CTNNB	Celastrus paniculatus	(a)155.70, (b)150.24, (c)131.85, (d)119.81, (e)141.57, (f)156.15, (g)148.58
5281525	(a)AXIN, (b)RAC	Acorus calamus	(a)64.31, (b)112.71

Note: The 32 hub genes, 16 resistant genes, and 23 VEGF pathway genes were docked against 557 phytochemicals from Medhya Rasayana plants using DS. The phytocompound with the best docking score for each target was identified and tabulated. The PubChem ID of phytocompounds, the target gene symbol, and corresponding plant name and LibDock score are presented. Targets: Hub genes: EGFR (7JXQ), IL6 (1ALU), VEGFA (1VPF), SRC (1A1C), CXCL8 (4XDX), IDH1 (4UMX), PTGS2 (5F19), ALDOA (5KY6), IL1B (5R7W), FGF2 (5X1O), HIF1A (4H6J), RHOQ (2ATX), ITGB1 (4WK0), CD44 (1UUH), SERPINE1 (1LJ5), TXNRD1 (2CFY), HMOX1 (6EHA), CYP1B1 (3PM0), PLAUR (3U74), TGM2 (3S3S), ITGAX (4NEH), NAMPT (4N9E), RARB (4DM6), HSPA1B (1HJO), THBS1 (1Z78), LOX (6TL7), NT5E (6Z9D), ATP2A2 (7BT2), IL6ST (1I1R), ALDH1A13 (7QK9), JAK1 (4E5W), PLOD2 (6TES). Resistant genes: FYN (2DQ7), PDGFRB (3MJG), ACVR1 (5S7K), RIPK2 (4C8B), PTPRR (2A8B), MMP3 (1UEA), F3 (1BOY), ITGA2 (1AOX), LY96 (2E56), NRP2 (2QQO), IL11 (4MHL), IL1A (2ILA), TIMP1 (2J0T), ZAK (6JUU), FLNC (3V8O), FGF13 (3HBW). VEGF pathway genes: VEGFR1 (3HNG), VEGFR2 (3VHE), NRP1 (1KEX), PKC Y (2UZP), RAS (5P21), RAF1 (1C1Y), MEK (3EQC), ERK (2Y9Q), PLC Y (4EY0), FAK (4I4E), CDC42 (2NGR), p38 (1W82), MAPK (3FHR), PI3K (3ZIM), RAC (1MH1), AKT (2X18), eNOS (3NOS), PXN (2VZI), Hsp27 (4MJH), AXIN (1EMU), GSK 3β (1Q3W), CTNNB (1LUJ), MMP9 (1L6J).

The total number of phytochemical docked against each target ranges from 18 to 552. Out of 557 phytochemicals, 14 phytochemicals gave top LibDock score with 23 targets as shown in Table 1. The phytochemical with PubChem ID 569889 docked with 7 targets eNOS, ERK, FAK, GSK 3β, MEK, VEGFR1, CTNNB; the phytochemical with PubChem ID 442774 (p38, VEGFR2), 197678 (MAPK, PI3K), and 5281525 (AXIN, RAC) docked with 2 targets each, and the remaining 10 phytochemicals docked with 1 target each.

Out of the 557 phytochemicals in Medhya Rasayana docked against 71 targets, 30 phytochemicals showed best interaction. The phytochemical with PubChem ID 569889 interacts with 27 targets, the phytochemical with PubChem IDs 197678 and 442774 interact with 5 targets each, the phytochemical with PubChem ID 31 interacts with 3 targets, and the phytochemicals with PubChem IDs 18016, 581589, 5281525, 131753027, and 54680871 interact with 2 targets each. Figure 2 shows the pie diagram of ligand and the number of interacting targets. 2D interaction images of docked complex were given as Supplementary Figure 1.

3.2. Network analysis of phytochemical-target interaction

3.2.1. Interaction of phytochemical with proteins expressed by hub genes

In Ayurveda, treatment is based on the individual's prakrithi type, where different plant combinations are used in the formulation as a personalized medicine. To further delineate the contribution of Medhya Rasayana plants and their phytochemical in reducing the resistance, a plant-phytochemical-target interaction network was generated. From the docking analysis of 557 phytocompounds with 32 hub genes, the top-scoring phytocompounds in each of the 13 plants were selected and a network was built.

The network incorporated 173 nodes and 890 edges, where the edges encoded interaction and the nodes represented potential targets (in red circle) or phytochemicals (in pink circle) and plant (in green squares). By using the centrality measurement of the network, it was found that the plants whose phytocompounds bind with all 32 targets
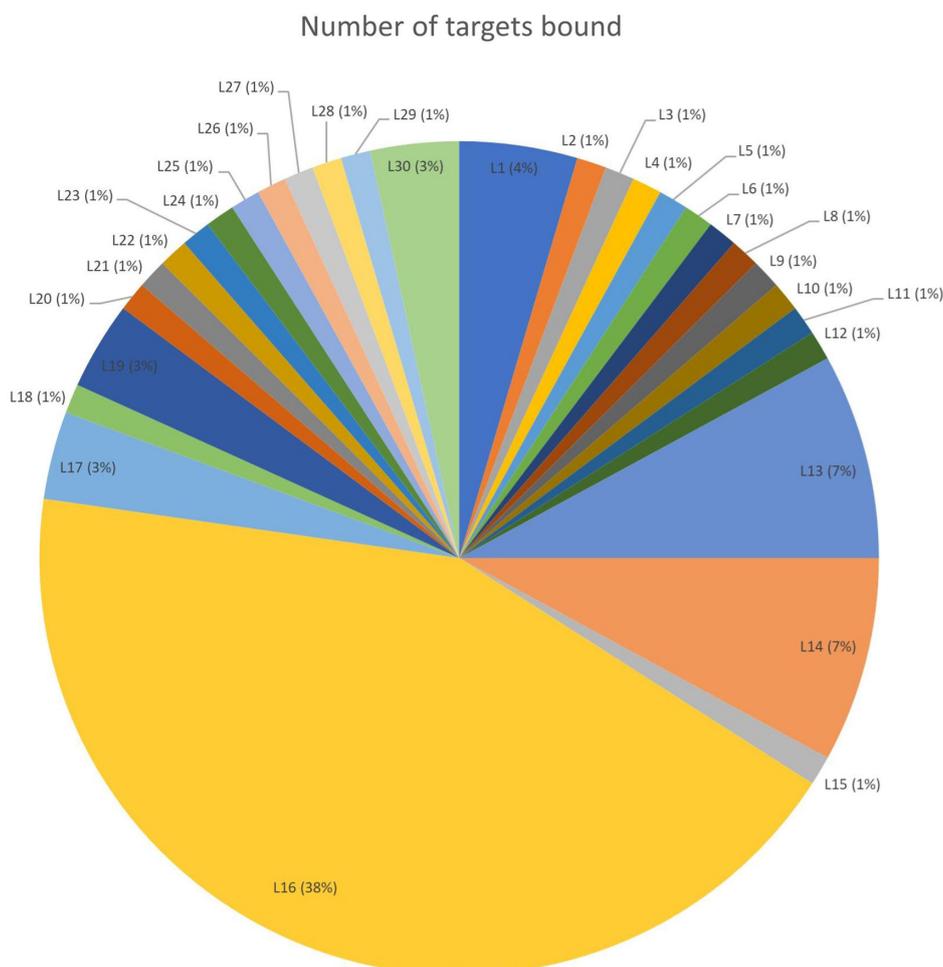

Figure 2. Pie diagram of ligand and the number of interacting targets. The phytochemical that gave the best docking score for each target was selected, and the number of targets of each phytochemical was identified and used to draw the pie diagram. The phytochemicals and the percentage of target (given in brackets) bound are represented. Ligand: PubChem ID L1: 31, L2: 965, L3: 3689, L4: 7991, L5: 10256, L6: 15608, L7: 18016, L8: 39378, L9: 61290, L10: 92776, L11: 97790, L12: 114829, L13: 197678, L14: 442774, L15: 538501, L16: 569889, L17: 581589, L18: 600601, L19: 5281525, L20: 5352449, L21: 5363633, L22: 5364942, L23: 5463146, L24: 6427087, L25: 6452096, L26: 20146588, L27: 131753027, L28: 235711, L29: 5312513, L30: 54680871.

are P1: Acorus calamus, P8: Evolvulus alsinoides, P9: Glycirrhiza glabra Linn, P10: Benincasa hispida (Figure 3). It is noteworthy to observe that the plant with minimum number of phytocompounds and maximum target interaction corresponds to P4: Celastrus paniculatus and P7: Convolvulus pluricaulis Choisy. Seven compounds in P4 showed interaction with 30 targets (Table 2).

3.2.2. Interaction of phytochemical with proteins expressed by resistant genes

From the docking analysis of 557 phytocompounds with 16 resistant genes, the top-scoring phytocompounds in each of the 13 plants were selected and a network built. As shown in Figure 4, the network consists of 104 nodes and 461 edges, where the
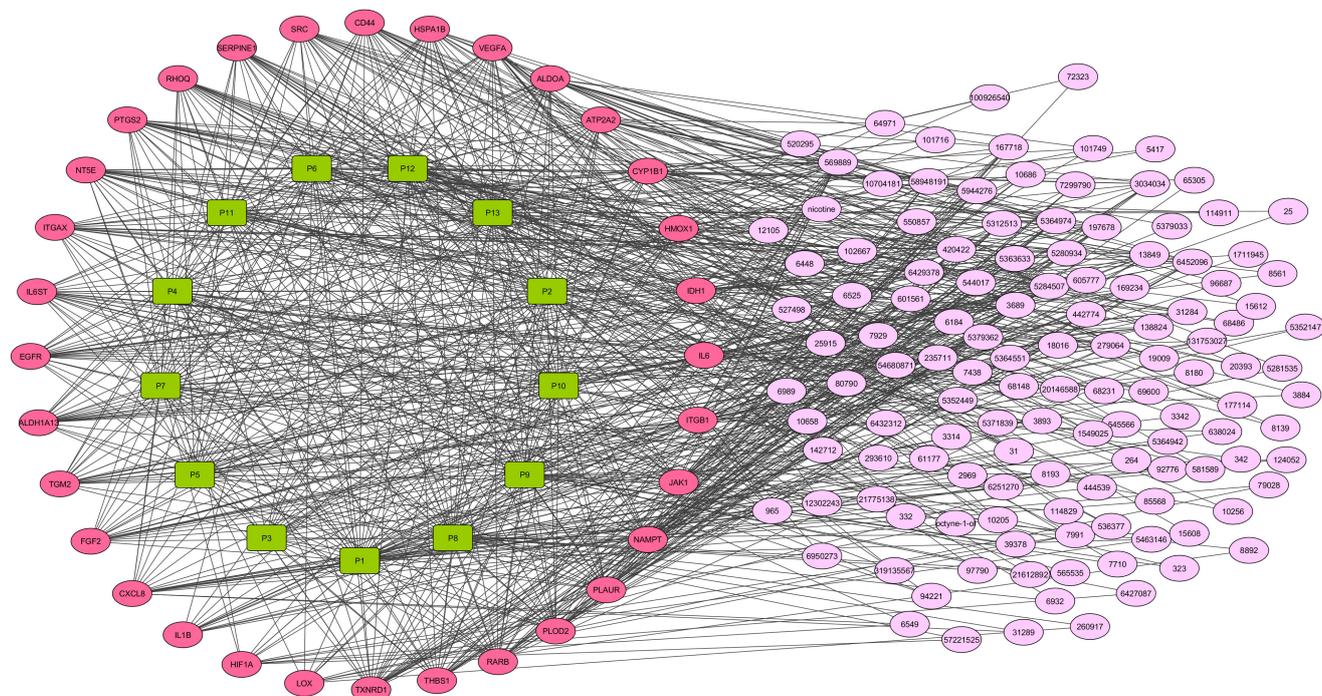
Figure 3. Interaction network between hub genes, phytochemicals, and plants. The plant-phytochemical-target interaction of hub genes was constructed using Cytoscape. The top-scoring phytocompounds in each of the 13 plants against each target were selected for the analysis. Red circles represent hub genes, pink circle represents phytochemicals, and green square represents plants. P1: Acorus calamus, P2: Bacopa monniera, P3: Canscora decussate, P4: Celastrus paniculatus, P5: Centella asiatica Linn, P6: Clitoria ternatea, P7: Convolvulus pluricaulis Choisy, P8: Evolvulus alsinoides, P9: Glycirrhiza glabra Linn, P10: Benincasa hispida, P11: Nardostachys jatamansi, P12: Plumbago zeylanica, P13: Tinospora cordifolia.

Table 2. Network analysis of selected hub genes, resistant genes, VEGF pathway genes, and phytochemicals in Medhya Rasayana plants

Plant	Degree			No: of phytochemical			No: of target		
	Hub	Resistant	VEGF	Hub	Resistant	VEGF	Hub	Resistant	VEGF
P1:Acorus calamus	50	26	34	18	11	13	32	15	21
P10:Benincasa hispida	41	20	25	10	5	6	32	15	19
P11:Nardostachys jatamansi	38	20	27	10	5	7	28	15	20
P12:Plumbago zeylanica	41	21	26	12	6	6	29	15	20
P13:Tinospora cordifolia	41	20	27	11	5	6	30	15	21
P2:Bacopa monniera	41	20	32	10	6	10	31	14	22
P3:Canscora decussate	23	19	19	4	4	3	19	15	16
P4:Celastrus paniculatus	37	20	27	7	5	6	30	15	21
P5:Centella asiatica Linn	33	18	26	6	4	5	27	14	21
P6:Clitoria ternatea	40	21	30	10	6	8	30	15	22
P7:Convolvulus pluricaulis Choisy	36	19	26	5	5	5	31	14	21
P8:Evolvulus alsinoides	47	21	30	15	6	8	32	15	22
P9:Glycirrhiza glabra Linn	46	25	34	14	9	12	32	16	22

Note: The plant-phytochemical-target interaction network for hub genes was generated using Cytoscape tool. The top-scoring phytocompounds in each of the 13 plants against each target were selected for the analysis and calculated the degree centrality using cytoNCA plugin in cytoscape. The degree centrality of each plant and the number of interacting phytochemicals and targets are presented.
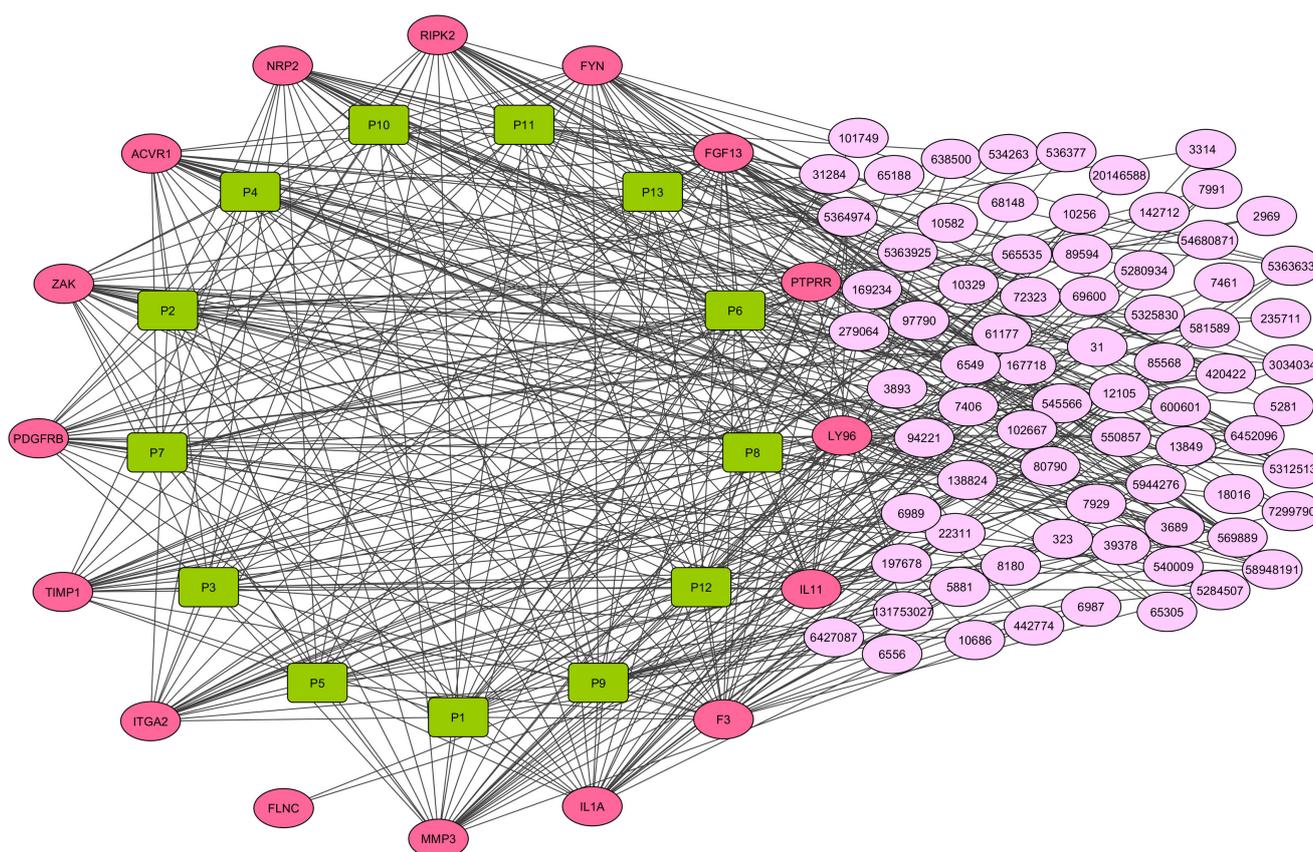
Figure 4. Interaction network between resistant genes, phytochemicals, and plants. The plant-phytochemical-target interaction network for the resistant genes was constructed using Cytoscape. The top-scoring phytocompounds in each of the 13 plants against each target were selected for the analysis. Red circles represent hub genes, pink circle represents phytochemicals, and green square represents plants. P1–P13 indicates the number of plants, and the names of each plant are detailed in legend in Figure 3.

edges encoded interaction and the nodes represented potential targets (in red circle) or phytochemicals (in pink circle) and plant (in green squares). It is found that the plants whose phytocompounds bind with maximum number of targets are P9: Glycirrhiza glabra Linn. Further, different phytocompounds in plants bound to almost all the resistant gene targets (Table 2).

3.2.3. Interaction of phytochemical with proteins expressed by VEGF pathway genes

From the docking analysis of 557 phytocompounds with 23 VEGF pathway genes, the top-scoring phytocompounds in each of the 13 plants were selected and a network built. As illustrated in Figure 5, the network incorporated 127 nodes and 627 edges, where the edges encoded interaction and the nodes represented potential targets (in red round shape) or phytochemicals (in pink circle) and plant (in circle). P9: Glycirrhiza glabra Linn, P2: Bacopa monniera, P6: Clitoria ternatea, P8: Evolvulus alsinoides bind to 22 targets.

The network pharmacological analysis revealed that, out of 13 plants in Medhya Rasayana, the phytochemicals of the plant Glycirrhiza glabra Linn bind to 70 targets followed by Evolvulus alsinoides 69 targets and Acorus calamus 68 targets. The plants that bind to 32 hub genes are Acorus calamus, Evolvulus alsinoides, Glycirrhiza glabra Linn, and Benincasa hispida. The plants that bind to 31 hub genes are Bacopa monniera and Convolvulus pluricaulis Choisy. Those with 30 hub genes are

Celastrus paniculatus, Clitoria ternatea, and Tinospora cordifolia. Also, the plant with least number phytochemical to cover the most number of targets is Celastrus paniculatus, and 10 phytochemicals interact with 66 targets (Table 2).

3.3. PE of phytocompounds of Medhya Rasayana plants

The docking results were further used to calculate the PE of individual phytocompound of Medhya Rasayana. This was done to assess the therapeutic potential of a phytochemical in the anti-VEGF-resistant condition. A threshold docking score value was set as 46.5 to filter out better docking poses, and the sum of the docking scores of a ligand to different targets represented its PE. A summary of the PE of the 30 ligands is given in Table 3. The phytochemicals with PubChem IDs 569889 have the highest PE 5690.88. The PE of Medhya Rasayana comprising of all the 13 plants against selected targets which was calculated by summing up the highest LibDock score of individual targets with 30 phytochemicals was found to be 7987.32.

The PE of individual plants in Medhya Rasayana was also calculated by summing up the highest score obtained for the phytochemicals of the respective plant against each target (Table 4). The plant Tinospora cordifolia has the highest PE followed by Glycirrhiza glabra Linn and Celastrus paniculatus.
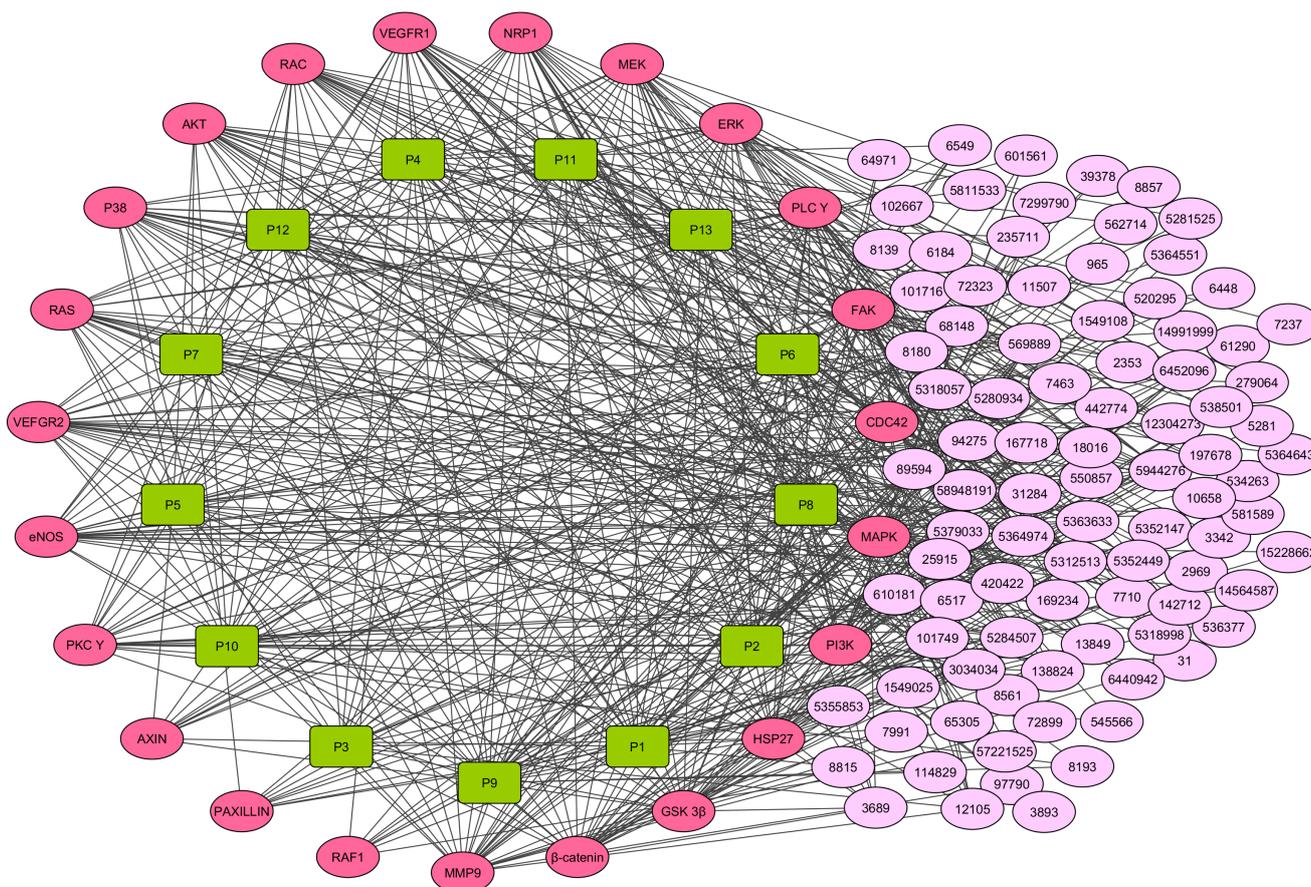
Figure 5. Interaction network between VEGF pathway genes, phytochemicals, and plants. The plant-phytochemical-target interaction of VEGF pathway genes was constructed using Cytoscape. The top-scoring phytocompounds in each of the 13 plants against each target were selected for the analysis. Red circles represent hub genes, pink circle represents phytochemicals, and green square represents plants. P1–P13 indicates the number of plants, and the names of each plant are detailed in legend in Figure 3.

Table 3. Prediction efficacy of Medhya Rasayana and the 30 individual phytochemicals obtained from the docking analysis with 71 targets

Ligand (PubChem ID)	Prediction efficacy
31	4693.22
965	5407.97
3689	4657.27
7991	2961.38
10256	3848.88
15608	4938.26
18016	5344.40
39378	3532.47
61290	3920.29
92776	4324.20
97790	4326.30
114829	3909.40
197678	4855.24
442774	4786.41
538501	3935.32
569889	5690.88
581589	5168.19

(*Continued*)

Table 3. (*Continued*)

Ligand (PubChem ID)	Prediction efficacy
600601	3693.43
5281525	4592.45
5352449	4922.98
5363633	5164.19
5364942	4243.06
5463146	4159.13
6427087	4327.07
6452096	4148.26
20146588	3187.76
131753027	4890.55
235711	5117.24
5312513	5208.07
54680871	3624.77
Prediction Efficacy of Medhya Rasayana	7987.32

Note: The prediction efficacy of each phytochemical was calculated by adding the LibDock score obtained from docking analysis with 71 targets. The PE of Medhya Rasayana was calculated by adding the highest LibDock score of individual targets with 30 phytochemicals. The PubChem ID and the prediction efficacy of 30 phytochemicals and the PE of the formulation with all the 13 herbs are presented.

Table 4. Prediction efficacy of plants in Medhya Rasayana

Plant number	Plant name	Prediction efficacy
P1	Acorus calamus	6952.08
P2	Bacopa monniera	6764.21
p3	Canscora decussate	3251.41
P4	Celastrus paniculatus	7341.40
P5	Centella asiatica Linn	5275.64
P6	Clitoria ternatea	6048.57
P7	Convolvulus pluricaulis Choisy	5987.14
P8	Evolvulus alsinoides	7047.15
P9	Glycirrhiza glabra Linn	7472.34
P10	Benincasa hispida	6300.22
P11	Nardostachys jatamansi	5255.50
P12	Plumbago zeylanica	6299.99
P13	Tinospora cordifolia	7697.90

Note: The prediction efficacy of plants in Medhya Rasayana was calculated by adding the highest score of phytochemicals from each plant against each target. The plant number, scientific name of the plant and the prediction efficacy were listed.

4. Discussion

Targeting angiogenesis has been a useful strategy to arrest tumor growth. One of the potential strategies for blocking angiogenesis is anti-VEGF therapy where the effect of the potent angiogenic factor and VEGF of tumor origin on endothelial cells could be blocked [13]. Blocking VEGF results in down-regulation of predominantly VEGF/ VEGFR2 signaling pathway. However, certain tumors develop resistance to anti-VEGF therapy and develop capillaries into the tumor site leading to the growth of the tumor. This anti-VEGF resistance is apparently due to alternative mechanisms leading to VEGFR2 activation and signaling in a VEGF-independent manner [14]. It can also be due to activation of other signaling pathways which link with the downstream components of VEGF/VEGFR2 signaling pathway. An alternative strategy in such situations would be to target key components of such pathways complementing anti-VEGF therapy. In the present study, we demonstrate the potential of such an approach to target differentially expressed genes in anti-VEGF-resistant GBMs by computationally predicting phytocompounds leveraging the traditional knowledge on medicinal plants that are employed in Ayurvedic formulations that are used against neurological diseases.

Herbal medicines play an important role in the management of several pathological conditions. Medhya Rasayana plants are used in Ayurvedic formulations which are beneficial for managing neurological disorders. It consists of 13 medicinal plants, all of which are known to possess neuroprotective activity as demonstrated in different experimental studies [15]. However, the antiangiogenic effect of Medhya Rasayana is still being explored. As indicated before, in resistance condition, by blocking of VEGF along with inhibition of the genes involved in alternative pathway of angiogenesis, progression of tumor might be inhibited. Based on these facts, an assumption was made that the active components present in the plants of this formulation could have the potential to reduce anti-VEGF resistance in GBM. The Medhya Rasayana phytochemicals were obtained from an internal phytochemical library. Out of 1973 phytochemicals from Medhya Rasayana plants, 557 phytochemicals pass both the Lipinski's rule and the BBB penetration potential. 71 target proteins were selected for studying the possible interaction of these phytochemicals through in silico molecular docking analysis. These 71 targets included (a) 13 receptors such as F3, PDGFRB, ITGB1, PLAUR, EGFR, and NRP2, (b) 20 enzymes including PTGS2, IDH1, ALDOA, ATP2A2, and (c) 7 ligands FGF2, IL6, IL11, THBS1, VEGFA, TGM2, SERPINE1, and (d) 15 were growth factors. Also, these targets were associated with pathways in cancer and significantly involved in positive regulation of angiogenesis and negative regulation of apoptosis.

Using LibDock of DS, 557 phytocompounds of Medhya Rasayana plants were docked against 71 targets. LibDock predicts the nature of molecular interaction between molecules and estimates the binding affinity of small molecules to the targets in terms of shape complementarity and hot spot identification [16]. Higher LibDock score is indicative of better ligand binding. The compounds showing the best docking score to each target were selected as the lead molecule. From the 557 phytochemicals docked, 30 phytochemicals showed better interaction to selected 71 targets. The binding of phytochemicals may inhibit the activity of target hub gene proteins and anti-VEGF-resistant proteins as these phytochemicals interact with some of the key residues to which standard inhibitor compound binds. PubChem ID 569889 and the corresponding reference drugs interact with some of the common residues in the inhibitor binding site and active site of different targets. PubChem ID 197678 and the reference inhibitor drug cefotaxime interact with 4 common residues in the inhibitor binding site of HMOX1. PubChem ID 131753027 and drug ropivacaine bind to 5 common residues in the ligand binding site of ITGB1. These 30 phytochemicals were present in nine plants such as Acorus calamus, Tinospora cordifolia, Evolvulus alsinoides, Glycirrhiza glabra Linn, Celastrus paniculatus, Plumbago zeylanica, Benincasa hispida, Bacopa monniera, and Convolvulus pluricaulis Choisy out of 13 plants in Medhya Rasayana. The pharmacological effects of most of these phytochemicals include anti-inflammatory and anti-cancer activity [17–26]. In vivo studies showed that the compound Liquiritigenin (PubChem ID 114829) has anti-cancer activity and also the ability to down regulate the expression, and secretion of VEGF was proved through in vitro and in vivo studies [27].

Molecular docking studies revealed that a single phytocompound binds to different targets though with varying binding affinity as indicated by their docking score. The compound Dihydrotestosterone 3-Formate-17-Benzoate (PubChem ID 569889) from the plant Celastrus paniculatus binds with 27 targets which include 7 receptors (F3, ITGAX, ACVR1, PLAUR, EGFR, NT5E and NRP2) and 11 enzymes (ALDOA, ATP2A2, CYP1B1, IDH1, JAK1, NAMPT, NT5E, PTGS2, TXNRD1, ACVR1, and FYN). The compound Hispaglabridin A (PubChem ID 442774) interacts with 1 enzyme, RIPK2, and 1 receptor LY96. The compound (2, 3, 4-trihydroxy-3-methylbutyl) dihydrogen phosphate (PubChem ID 31) interacts with 3 targets of which ITGA2 is a receptor and TIMPI a regulator of enzyme critical to growth. The compound Shinflavanone (PubChem ID 197678) interacts with 5 targets of which ALDH1A13 and HMOX1 are enzymes and THBS1 is a growth factor. These results indicate that the compounds that bind to greater number of receptors and enzymes as shown by their docking score may have therapeutic potential in overcoming anti-VEGF resistance.

As several phytocompounds of Medhya Rasayana plants showed binding to different key targets, the therapeutic potential of such ligands was assessed by predicting the efficacy of each of these phytocompounds by summing up the docking scores of each ligand against different targets. The compound Dihydrotestosterone 3-Formate-17-Benzoate showed highest

efficacy followed by compounds such as 9-Octadecenoic Acid (PubChem ID 965), Dibutyl Azelate (PubChem ID 18016), and Cis-10-Nonadecenoic Acid (PubChem ID 5312513). The targets of these compounds include hub genes such as IL1B, FGF2, EGFR, IDH1, PTGS2, ALDOA, PLAUR, VEGF pathway genes such as PXN, PLC Y, VEGFR1, NRP2, MEK, and FAK, and resistance genes such as FYN, ACVR1, F3, NRP2, IL11, ZAK, FGF13 that are involved in cancer pathways and angiogenesis process. Dihydrotestosterone 3-Formate-17-Benzoate (PubChem ID 569889) from the plant Celastrus paniculatus binds with 27 targets such as ALDOA, ATP2A2, CYP1B1, EGFR, IDH1, ITGAX, JAK1, NAMPT, NT5E, PLAUR, PLOD2, PTGS2, TXNRD1, ACVR1, F3, FYN, IL11, NRP2, ZAK, FGF13, eNOS, ERK, FAK, GSK 3β, MEK, VEGFR1, and CTNNB which includes 13 hub genes, 7 resistant genes, and 7 VEGF pathway genes. Dihydrotestosterone 3-Formate-17-Benzoate binds at the receptor kinase domain of EGFR [28] with a LibDock score of 148.13. It binds at the active site of PTGS2, the site where the drug aspirin binds [29], with a LibDock score 136.74. It is also docked at the active site of PLAUR [30] with a LibDock score 163.06. It is therefore possible that the binding of these molecules to the targets may affect the activity of these targets.

Among the 30 phytochemicals that bind to the 71 targets, Dihydrotestosterone 3-Formate-17-Benzoate bound with 38% (27 targets) of the targets, followed by Shinflavanone (PubChem ID 197678) and Hispaglabridin A (PubChem ID 442774) that docked to 7% targets (5 each) and (2,3,4-trihydroxy-3-methylbutyl) dihydrogen phosphate (PubChem ID 31) bound with 4% (3 targets). This raises the possibility of exploring the potential of such phytocompound as a potential agent against anti-VEGF resistance in GBM.

The results presented here based on the binding of multiple phytocompounds from different Medhya Rasayana plants with multiple targets involved in resistance to anti-VEGF therapy in GBM are particularly relevant in the context of Ayurveda concept of therapy. Formulations of multiple medicinal plants containing multiple phytocompounds are prescribed in a personalized manner depending on the "biological constitution" (prakrithi) of each individual, rather than a monotherapy, facilitating multi-target therapy. Each medicinal plant belonging to Medhya Rasayana group contains multiple phytocompounds that show binding affinity to different targets as demonstrated by LibDock score of each pair. PE of each plant in Medhya Rasayana was calculated, and the plant Tinospora cordifolia has highest efficacy (7697.90) followed by Glycirrhiza glabra Linn (7472.34), Celastrus paniculatus (7341.40) and Evolvulus alsinoides (7047.15). The PE of Medhya Rasayana was calculated by summing up the highest docking score obtained for each target with 30 phytocompound, which was found to be 7987.32.

Similar results on the efficacy of each plant were also obtained by network analysis of phytochemicals of each plant with various targets. By such an analysis of individual plants, the plant Glycirrhiza glabra Linn was found to show greater potential. Phytochemicals of this plant bind to all the selected targets except PXN belonging to VEGF pathway and include all the 32 hub genes and 16 resistant genes, 22 VEGF pathway gene. The phytochemicals of the plant Evolvulus alsinoides bind to 69 targets, which include 32 hub genes, 15 resistant genes except 1 (FLNC), and 22 VEGF pathway genes except 1; in the case of Acorus calamus, 68 targets were found to bind with the phytochemicals, while in the case of Tinospora cordifolia and Celastrus paniculatus, 66 targets could bind with plant phytochemicals.

By evaluating the relative efficacy of each plant against the different targets predicted to be contributing to anti-VEGF resistance, it could be possible to predict combinations of the herbs, for Ayurvedic formulations against anti-VEGF resistance, consistent with the "prakrithi" concept of Ayurveda. A combination of phytochemicals of Glycirrhiza glabra Linn, Evolvulus alsinoides, and Celastrus paniculatus would be more effective in targeting all the anti-VGEF resistant proteins.

In cancer, adjuvant therapy is an additional treatment given to patients either along with or after the main treatment procedure. The primary goal of adjuvant therapy is to improve disease-free and OS by targeting micro-metastatic and residual disease. The advantage of adjuvant therapy includes increased chance of disease-free survival, a decreased chance of recurrence, or added life-years. Hence, the potential of using formulation containing Medhya Rasayana plants specifically Glycirrhiza glabra Linn and Celastrus paniculatus, which has been hitherto used for treating Neurological disorders, as an adjuvant therapy along with anti-VEGF therapy is a promising approach.

5. Conclusion

The present study suggest the scope of developing a patient-specific formulation using selected Medhya Rasayana plants, probably as an adjuvant therapy along with anti-VEGF therapy against GBM. Further in vitro and in vivo experimental studies are required to validate the in silico prediction results, before it can be taken for clinical studies.

Conflicts of Interest

The authors declare that they have no conflicts of interest to this work.

Data Availability Statement

The data that support this work are available upon reasonable request to the corresponding author.

Author Contribution Statement

References

[1] Soumya, S. J., Arya, K. R., Abhinand, C. S., Sunitha, P., Athira, A. P., Nair, A. S., . . . , & Sudhakaran, P. R. (2024). Multi-target and natural product-based multi-drug approach for anti-VEGF resistance in glioblastoma. *Exploration of Drug Science*, *2*(5), 567–582. https://doi.org/10.37349/eds.2024.00062

[2] Soda, Y., Myskiw, C., Rommel, A., & Verma, I. M. (2013). Mechanisms of neovascularization and resistance to anti-angiogenic therapies in glioblastoma multiforme. *Journal of Molecular Medicine*, *91*, 439–448. https://doi.org/10.1007/s00109-013-1019-z

[3] Piao, Y., Liang, J., Holmes, L., Henry, V., Sulman, E., & de Groot, J. F. (2013). Acquired resistance to anti-VEGF therapy in glioblastoma is associated with a mesenchymal transition. *Clinical Cancer Research*, *19*(16), 4392–4403. https://doi.org/10.1158/1078-0432.CCR-12-1557

[4] Pineda, E., Domenech, M., Hernández, A., Comas, S., & Balaña, C. (2023). Recurrent glioblastoma: Ongoing clinical challenges and future prospects. *OncoTargets and Therapy*, *16*, 71–86. https://doi.org/10.2147/OTT.S366371

[5] Kawabata, S., Suzuki, M., Hirose, K., Tanaka, H., Kato, T., Goto, H., . . . , & Miyatake, S. I. (2021). Accelerator-based BNCT for patients with recurrent glioblastoma: A multicenter phase II study. *Neuro-Oncology Advances*, *3*(1), vdab067. https://doi.org/10.1093/noajnl/vdab067

[6] Weathers, S. P., & de Groot, J. (2015). VEGF manipulation in glioblastoma. *Oncology*, *29*(10), 720–727.

[7] Taylor, O. G., Brzozowski, J. S., & Skelding, K. A. (2019). Glioblastoma multiforme: An overview of emerging therapeutic targets. *Frontiers in Oncology*, *9*, 963. https://doi.org/10.3389/fonc.2019.00963

[8] Arya, K. R., Bharath Chand, R. P., Abhinand, C. S., Nair, A. S., Oommen, O. V., & Sudhakaran, P. R. (2021). Identification of hub genes and key pathways associated with anti-VEGF resistant glioblastoma using gene expression data analysis. *Biomolecules*, *11*(3), 403. https://doi.org/10.3390/biom11030403

[9] Ramawat, B., Jangid, V., & Samagandi, K. (2022). Review article on the role of Medhya Rasayana: Enhancing the intellectual power. *Journal of Ayurveda and Integrated Medical Sciences*, *7*(5), 69–74. https://jaims.in/jaims/article/view/1882

[10] Sunitha, P., Raju, R., Sajil, C. K., Abhinand, C. S., Nair, A. S., Oommen, O. V., . . . , & Sudhakaran, P. R. (2019). Temporal VEGFA responsive genes in HUVECs: Gene signatures and potential ligands/receptors fine-tuning angiogenesis. *Journal of Cell Communication and Signaling*, *13*, 561–571. https://doi.org/10.1007/s12079-019-00541-7

[11] Lipinski, C. A., Lombardo, F., Dominy, B. W., & Feeney, P. J. (2012). Experimental and computational approaches to estimate solubility and permeability in drug discovery and development settings. *Advanced Drug Delivery Reviews*, *64*, 4–17. https://doi.org/10.1016/j.addr.2012.09.019

[12] Butina, D., Segall, M. D., & Frankcombe, K. (2002). Predicting ADME properties in silico: Methods and models. *Drug Discovery Today*, *7*(11), S83–S88. https://doi.org/10.1016/S1359-6446(02)02288-2

[13] Liu, Z. L., Chen, H. H., Zheng, L. L., Sun, L. P., & Shi, L. (2023). Angiogenic signaling pathways and anti-angiogenic therapy for cancer. *Signal Transduction and Targeted Therapy*, *8*(1), 198. https://doi.org/10.1038/s41392-023-01460-1

[14] Qi, S., Deng, S., Lian, Z., & Yu, K. (2022). Novel drugs with high efficacy against tumor angiogenesis. *International Journal of Molecular Sciences*, *23*(13), 6934. https://doi.org/10.3390/ijms23136934

[15] Acharya, V. J. T. (1941). *Charaka Samhita (Sanskrit) of Agnivesha with Ayurveda Dipika commentary*. India: Nirnaya Sagar Press.

[16] Rao, S. N., Head, M. S., Kulkarni, A., & LaLonde, J. M. (2007). Validation studies of the site-directed docking program LibDock. *Journal of Chemical Information and Modeling*, *47*(6), 2159–2171. https://doi.org/10.1021/ci6004299

[17] Beschi, D. A., Appavoo, M. R., & Wilsy, J. I. (2021). GC-MS analysis, collected from Kavalkinaru area, Tirunelveli district, Tamil Nadu, India. *European Journal of Molecular & Clinical Medicine*, *8*(11), 2021.

[18] Jayaraj, R. L., Beiram, R., Azimullah, S., Mf, N. M., Ojha, S. K., Adem, A., & Jalal, F. Y. (2020). Valeric acid protects dopaminergic neurons by suppressing oxidative stress, neuroinflammation and modulating autophagy pathways. *International Journal of Molecular Sciences*, *21*(20), 7670. https://doi.org/10.3390/ijms21207670

[19] Han, R., Nusbaum, O., Chen, X., & Zhu, Y. (2020). Valeric acid suppresses liver cancer development by acting as a novel HDAC inhibitor. *Molecular Therapy-Oncolytics*, *19*, 8–18. https://doi.org/10.1016/j.omto.2020.08.017

[20] Chen, H., Tang, X., Liu, T., Jing, L., & Wu, J. (2019). Zingiberene inhibits *in vitro* and *in vivo* human colon cancer cell growth via autophagy induction, suppression of PI3K/AKT/mTOR Pathway and caspase 2 deactivation. *Journal of BUON*, *24*(4), 1470–1475.

[21] Ashokkumar, K., Murugan, M., Dhanya, M. K., Sathyan, T., Raj, S., & Mathews, N. (2020). Traditional uses, phytochemistry, and pharmacological properties of Zingiber officinale essential oil and extracts. In N. Mishra (Ed.), *Ethnopharmacological investigation of Indian spices* (pp. 62–84). IGI Global. https://doi.org/10.4018/978-1-7998-2524-1.ch005

[22] Wang, Z. F., Liu, J., Yang, Y. A., & Zhu, H. L. (2020). A review: The anti-inflammatory, anticancer and antibacterial properties of four kinds of licorice flavonoids isolated from licorice. *Current Medicinal Chemistry*, *27*(12), 1997–2011. https://doi.org/10.2174/0929867325666181001104550

[23] Alibakhshi, A., Malekzadeh, R., Hosseini, S. A., & Yaghoobi, H. (2023). Investigation of the therapeutic role of native plant compounds against colorectal cancer based on system biology and virtual screening. *Scientific Reports*, *13*(1), 11451. https://doi.org/10.1038/s41598-023-38134-5

[24] Fukuzawa, M., Yamaguchi, R., Hide, I., Chen, Z., Hirai, Y., Sugimoto, A., . . . , & Nakata, Y. (2008). Possible involvement of long chain fatty acids in the spores of *Ganoderma lucidum* (Reishi Houshi) to its anti-tumor

activity. *Biological and Pharmaceutical Bulletin*, *31*(10), 1933–1937. https://doi.org/10.1248/bpb.31.1933

[25] El-Sawy, E., Abo-Salem, H., & Mandour, A. (2017). 1H-Indole-3-carboxaldehyde: Synthesis and reactions. *Egyptian Journal of Chemistry*, *60*(5), 723–751. https://doi.org/10.21608/ejchem.2017.1097.1053

[26] Bouone, Y. O., Bouzina, A., Sayad, R., Djemel, A., Benaceur, F., Zoukel, A., . . . , & Bouchareb, F. (2023). $BiCl_3$-catalyzed green synthesis of 4-hydroxy-2-quinolone analogues under microwave irradiation. *RSC Advances*, *13*(40), 28030–28041. https://doi.org/10.1039/D3RA05289C

[27] Liu, Y., Xie, S., Wang, Y., Luo, K., Wang, Y., & Cai, Y. (2012). Liquiritigenin inhibits tumor growth and vascularization in a mouse model of HeLa cells. *Molecules*, *17*(6), 7206–7216. https://doi.org/10.3390/molecules17067206

[28] Stamos, J., Sliwkowski, M. X., & Eigenbrot, C. (2002). Structure of the epidermal growth factor receptor kinase domain alone and in complex with a 4-anilinoquinazoline inhibitor. *Journal of Biological Chemistry*, *277*(48), 46265–46272. https://doi.org/10.1074/jbc.M207135200

[29] Lucido, M. J., Orlando, B. J., Vecchio, A. J., & Malkowski, M. G. (2016). Crystal structure of aspirin-acetylated human cyclooxygenase-2: Insight into the formation of products with reversed stereochemistry. *Biochemistry*, *55*(8), 1226–1238. https://doi.org/10.1021/acs.biochem.5b01378

[30] Llinas, P., Hélène Le Du, M., Gårdsvoll, H., Danø, K., Ploug, M., Gilquin, B., . . . , & Ménez, A. (2005). Crystal structure of the human urokinase plasminogen activator receptor bound to an antagonist peptide. *The EMBO Journal*, *24*(9), 1655–1663. https://doi.org/10.1038/sj.emboj.7600635

Supplementary File

Supplementary Figure 1. 2D interaction images of potent target-ligand docked complex.
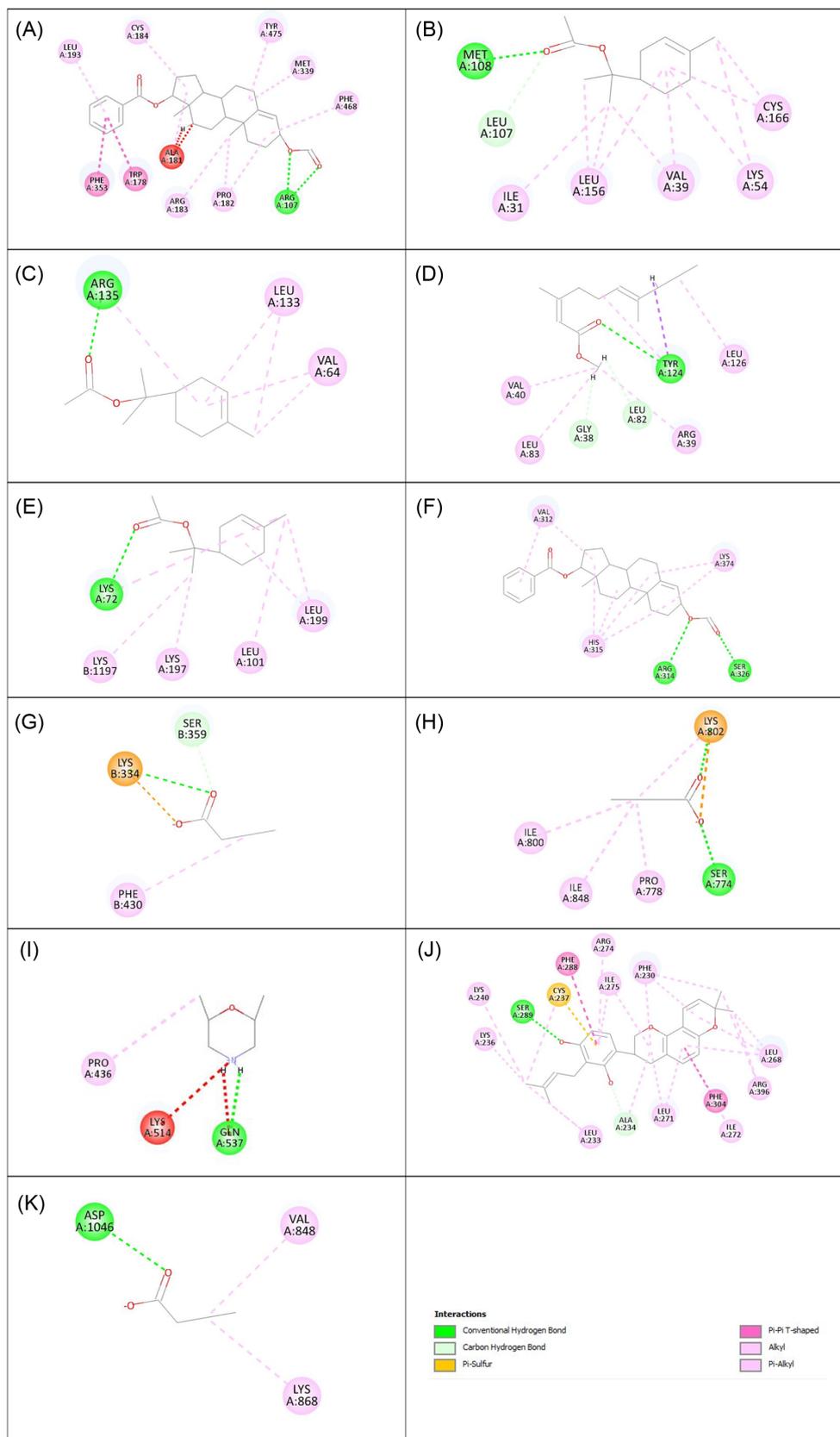
(A) ENOS-569889, (B) ERK-569889, (C) F3-569889, (D) FGF2-18016, (E) FGF13-569889, (F) IDH1-569889, (G) ITGB1-131753027, (H) PI3K-197678, (I) PTPRR-13175302, (J) RARB-442774, (K) VEGFR2-442774.